SU-SEL-64-061

Phase Height Oscillations in the Ionosphere

by
Theodore M. Watt

April 1964

Technical Report No. 7

Prepared under
National Aeronautics and Space Administration
Contract NsG 30-60

Technical Report No. 95

Prepared under
Office of Naval Research Contract
Nanr-225(64), NR 088 019, and
Advanced Research Projects Agency ARPA Order 196-63

RADIOSCIENCE LABORATORY

STANFORD ELECTRONICS LABORATORIES

STANFORD UNIVERSITY · STANFORD, CALIFORNIA

SEL-64-061

PHASE HEIGHT OSCILLATIONS IN THE IONOSPHERE

by

Theodore M. Watt

April 1964

Technical Report No. 7

Prepared under
National Aeronautics and Space Administration
Contract NsG 30-60

and

Technical Report No. 95

Prepared under
Office of Naval Research Contract
Nonr-225(64), NR 088 019,
and
Advanced Research Projects Agency ARPA Order 196-63

Radioscience Laboratory
Stanford Electronics Laboratories
Stanford University Stanford, California

ABSTRACT

An account is given of an experiment which took place in Alberta, Canada, during the summer of 1963. The primary purpose of the experiment was to look for correlation between ionospheric phase height fluctuations and long period magnetic micropulsations with the thought that this correlation might be interpreted either in terms of hydromagnetic waves or as drift motions produced by E region currents. Atmospheric pressure fluctuations were also recorded for possible correlation studies.

The experimental equipment, techniques, and parameters are all described and consideration is given to those aspects of the experiment which might merit modification in any similar experiment in the future.

The data are compared in three ways:

1. Phase height -- micropulsations
2. Phase height -- atmospheric pressure
3. Ordinary wave -- Extraordinary wave phase height

Although positive correlation was not observed, it is shown how the lack of correlation could be attributed to certain definite causes which can be eliminated in any future experiment.

CONTENTS

TABLE OF FIGURES

ACKNOWLEDGMENTS

The advice of Professor Owen K. Garriott, under whose guidance this experiment was performed, is very much appreciated. Also appreciated are the many helpful discussions which took place with Dr. Henry Rishbeth and Professors O. G. Villard, Jr., and R. A. Helliwell. Mr. D. M. Annett accomplished much of the equipment installation. The use of Pacific Naval Laboratories equipment and the cooperation and assistance received from personnel of Suffield Experimental Station is gratefully acknowledged. This experiment was supported both by grants NsG-30-60 and Nonr 225(64).

I. INTRODUCTION

An interesting aspect of the study of the ionosphere is the consideration of wave propagation and structure. Hines[1] (1960) considers wave structure observed in rocket trails and interprets these observations in terms of internal atmospheric gravity waves. Using radio techniques, Chan[2] (1962) observed traveling ionospheric disturbances (TID's) and on several occasions noticed strong correlation between TID's and fluctuations in the earth's magnetic field. Rishbeth and Garriott[3] (1964) consider Chan's observations and interpret the correlation both in terms of the "dynamo-motor" theory and in terms of ionospheric hydromagnetic waves.

Any wave, whatever its character and origin, should cause motion of the plasma as it propagates through the ionosphere. It would appear then, that a method for sensing small, localized oscillations in the ionosphere would be an effective tool for the study of a variety of wave phenomena associated with the ionosphere.

A simple but highly sensitive cw phase height sounder has been developed, and the experiment herein described was set up around this device in an attempt to study the hypotheses noted above. Briefly, the technique is as follows: 1) Vertical motion of the ionosphere is measured by means of the phase sounder. 2) Magnetic field fluctuations are measured along three components. 3) Atmospheric pressure fluctuations are measured. Following the work of Hines, we look for correlation between 1) and 3). Following the work of Rishbeth and Garriott, we look for correlation between 1) and 2).

It is instructive to consider in greater detail the two types of waves which have been postulated, i.e., hydromagnetic waves and gravity waves.

A. HYDROMAGNETIC WAVES

A great deal is known about hydromagnetic waves from studies in plasma physics. In the paper by Rishbeth and Garriott, only the simplest form of hydromagnetic wave is considered, namely an Alfvén wave propagating along a magnetic field line. On the basis of this and certain other assumptions, an expression is derived which relates (vertical) plasma velocity to magnetic field fluctuations. The expression is

$$V_{ZH} = \Delta B \cot I \, (\omega/\nu_{in} \, \mu_o m_i N)^{\frac{1}{2}} \qquad (1)$$

in which V_{ZH} is the vertical velocity of the plasma, ΔB is the amplitude of the magnetic field fluctuation, I is the dip angle, ν_{in} is ionic collision frequency, μ_o is the permeability of free space, m_i is ionic mass, and N is electron number density. The significance of Eq. (1), for purposes of this experiment, lies in its prediction of proportionality between vertical plasma velocities and the amplitudes of magnetic field fluctuations. In Section III, this relationship is explored quantitatively, and expressions are derived predicting the relative amplitudes of the parameters to be measured in this experiment.

B. GRAVITY WAVES

The existence of atmospheric gravity waves may be postulated by considering the conditions which govern atmospheric oscillations. These conditions can be expressed in terms of three equations; the equations of motion, of adiabatic state, and of continuity. The simultaneous solutions of these equations predict the propagation of waves. Hines has solved these equations and shown that where gravity is neglected,

the solutions reduce to the ordinary solutions of sound propagation, and are therefore called "acoustic" waves. Under these conditions the equation relating wave frequency and speed is non dispersive, i.e., $\omega^2 = C^2K^2$, in which K is the associated wave number and C is the speed of sound.

In the presence of gravity, however, the solutions give rise to permissible values for ω which do not represent a continuous spectrum, but rather fall into two distinct regions. Only values of ω falling within these regions can represent propagating waves. Frequencies falling within these two regions are called ω_a and ω_g and are specified as:

$$\omega_a > \frac{\gamma g}{2C} \tag{2}$$

$$\omega_g < \frac{(\gamma-1)^{\frac{1}{2}}\, g}{2C} \tag{3}$$

Moreover, since γ, which is the usual ratio of specific heats, is always less than 2, then $\omega_a > \omega_g$ always. ω_a is associated with acoustic waves and ω_g is associated with another sequence of waves which have been labeled as "internal gravity waves."

In principle, values for ω_g can be arbitrarily small. Indeed, observations have indicated the existence of waves with periods of the order of 30 minutes for which the interpretation in terms of gravity waves poses interesting experimental possibilities.

II. DESCRIPTION OF EXPERIMENT

A. IONOSPHERIC PHASE SOUNDING

The phase sounder measures vertical motion of the ionosphere by measuring the modulating effect this motion has on a signal received from a source of precision frequency. Briefly, the operation is as follows: A cw signal is transmitted from a source which is driven by a frequency standard (accuracy one part in 10^8 per day). The resulting sky wave is reflected from the ionosphere and received at a recording site a short distance away (Figure 1). The received signal is compared with a reference signal controlled by another frequency standard and the instantaneous phase difference is recorded. In the absence of ionospheric motion, the summation of the received signal and the reference signal will result in a constant frequency difference. If the reference signal is adjusted such that the difference frequency is zero, then the phase difference will be unchanging with time.

Under these circumstances, the Doppler effect of vertical motion of the plasma will result in a phase modulation of the received signal which may be observed as a variation in the signal representing the phase difference.

A detailed explanation of the system operation is divided into four parts: Transmitter Operation, Ionospheric Effects, Receiver Operation and Signal Processing, and Phase-Height Parameters. These will now be considered in order.

1. Transmitter Operation

A self-explanatory block diagram of the transmitter system is shown in Figure 2. The four available frequencies were 2.0, 2.2, 4.0, and 4.4 Mc. Two antenna systems were employed with half wavelength center frequencies of 2.1 Mc and

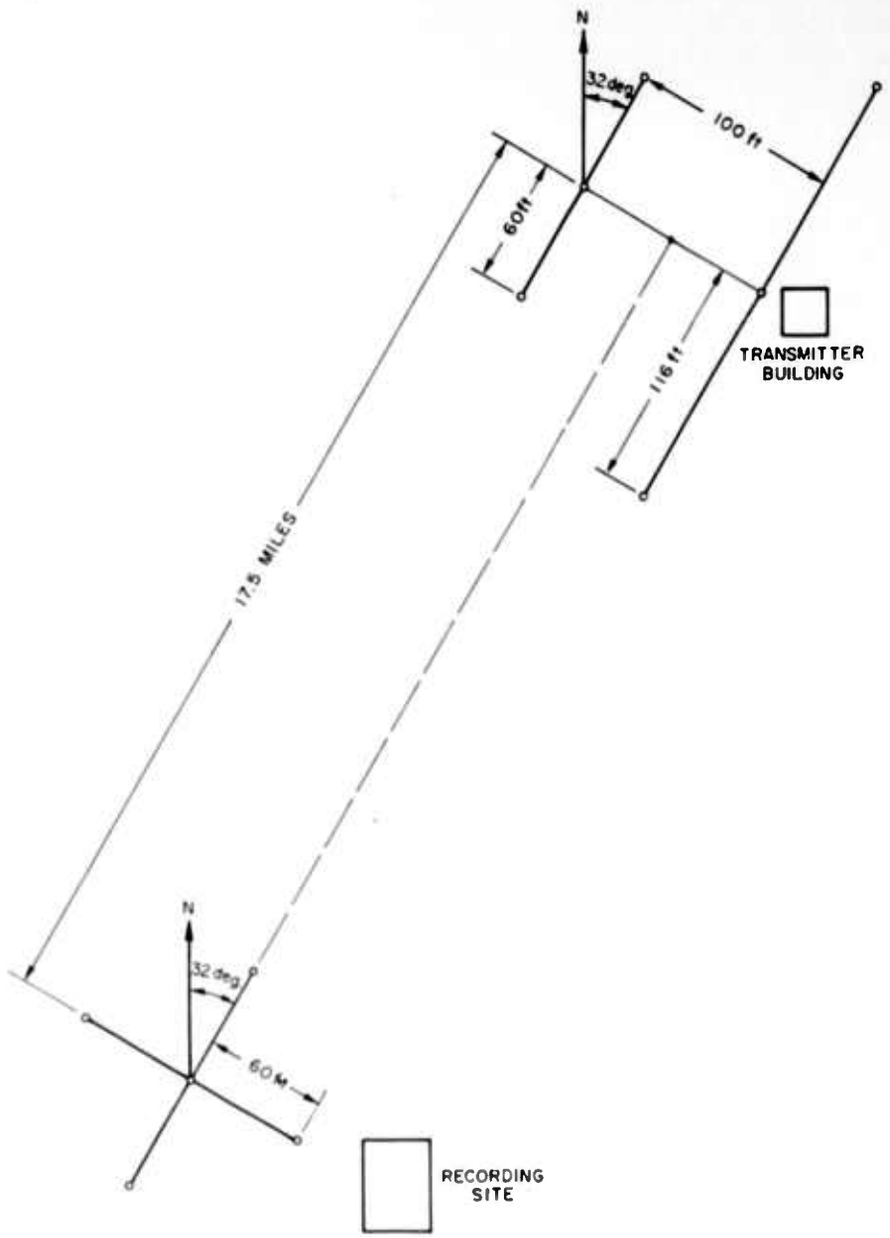

FIG. 1. PLAN VIEW OF EXPERIMENT SITE

4.2 Mc. The antenna impedance at 2.0 Mc turned out to be lower than expected, and this resulted in excessive loading of the transmitter. Consequently, 2.0 Mc was used very little.

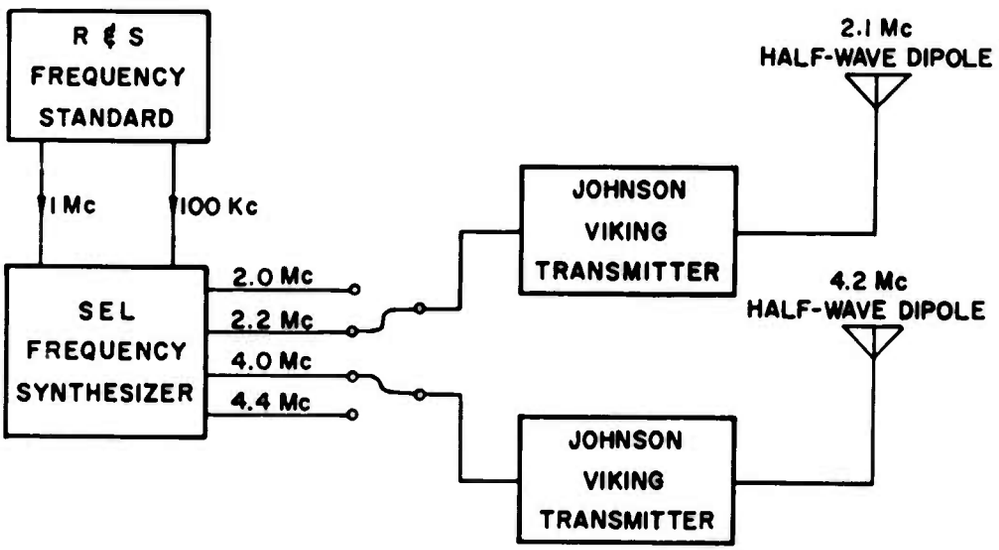

FIG. 2. PHASE SOUNDER TRANSMITTER SYSTEM

2. Ionospheric Effects

A sketch of idealized ray paths is shown in Figure 3. As shown in the sketch, the received signal may be considered as a summation of a sky wave S_1 and a ground wave S_2. Both S_1 and S_2 are of the form

$$S = A \cos(\omega t - \int_o^p \beta dp) \qquad (4)$$

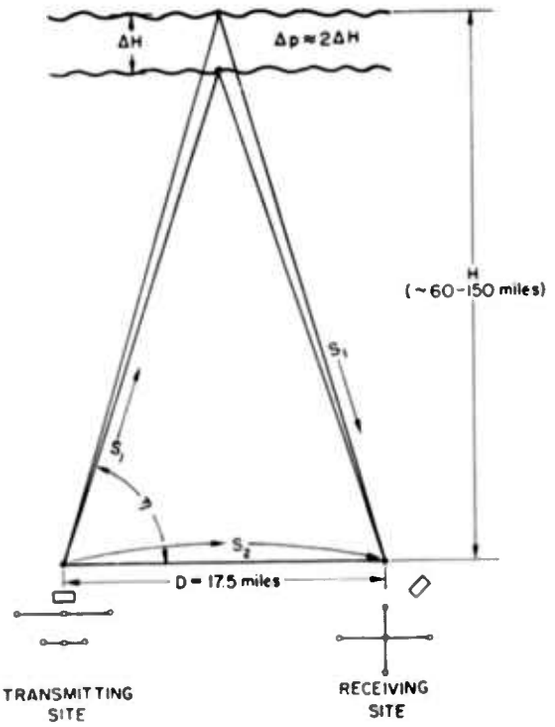

FIG. 3. PHASE SOUNDER PROPAGATION PATHS

as seen by the receiving antennas. Here dp is the incremental propagation path length and $\beta = \frac{2\pi}{\lambda}$ where λ is the wavelength. For the ground wave, the expression becomes

$$S_2 = A_2 \cos(\omega t - \beta_o D) \qquad (5)$$

in which $\beta_o = \frac{2\pi}{\lambda_o}$ where λ_o is the free space wavelength (constant). For the sky wave, β is a function both of space and time. However, we can define the refractive index of a medium as $\mu = \lambda_o/\lambda$ so that $\beta = \mu\beta_o$. The sky wave

signal is then given by

$$S_1 = A_1 \cos(\omega t - \beta_o \int_o^p \mu dp) \qquad (6)$$

The total signal S seen by the receiving antennas is therefore given by

$$S = S_1 + S_2 \qquad (7)$$

Under typical conditions, the 2.0 Mc and 2.2 Mc sky wave signals tended to be absorbed during daylight hours. Under these conditions, $A_1 << A_2$ and $S \approx S_2$. This provided a convenient means for calibrating the frequency standards. Except for this, however, the presence of a ground wave was a nuisance. In general, useful data was obtained only when $A_2 << A_1$ so that $S \approx S_1$.

We can greatly simplify the problem and yet not lose very much accuracy if we assume vertical incidence. This is approximately true as shown by Figure 3. On this basis, we can define a quantity "phase height" by the expression $H_1 = \frac{1}{2}\int_o^p \mu \, dp = \int_o^H \mu \, dh$ where $H = P/2$ and is considered to be the true height of reflection of the wave. We may now express S_1 as

$$S_1 = A_1 \cos(\omega t - 2\beta_o \int_o^H \mu dh) \qquad (8)$$

The frequency of S_1 is given by $(\omega - \frac{\partial}{\partial t}[2\beta_o \int_o^H \mu dh])$ and since ω is essentially constant, changes in frequency are due entirely to time variations in $(\int_o^H \mu dh)$. Unfortunately, the relationship is not easily expressed without making further simplifying assumptions. Specifically, assumptions must

be made with respect to μ as a function both of time and of height. The assumption we make which greatly simplifies the problem, but is reasonable from a physical point of view, is as follows: Ionization is not a continuous function of height, but exists only in a layer with a well defined lower boundary. A change in phase is caused by a vertical motion of the entire layer. The shape of the layer does not vary with time.

If we designate the bottom of the layer as H_b, we can say

$$\int_o^H \mu dh = \int_o^{H_b} \mu dh + \int_{H_b}^H \mu dh \qquad (9)$$

From the above assumption, $\int_o^{H_b} \mu dh = \int_o^{H_b} dh = H_b$ and $\int_{H_b}^H \mu dh$ is constant; therefore, $H_b = H$ minus a constant. We can now express S_1 as

$$S_1 = A_1 \cos(\omega t + \phi_1 - 2\beta_o H) \qquad (10)$$

where ϕ_1 is a constant.

3. Receiver Operation and Signal Processing

Operation of the receiving system may best be understood by referring to Figure 4. The signal $S = S_1 = A_1 \cos(\omega t - 2\beta_o H + \phi_1)$ is received by the master receiver as shown. The reference signal $S_3 = A_3 \cos(\omega t + \phi_3)$ is injected into the slave phase receiver by virtue of extracting an appropriate harmonic from a precision 100 kc signal. At this point, the phase difference between S_3 and S_1 is simply $\Delta\phi = \phi_3 - \phi_1 + 2\beta_o H$. S_1 and S_3 are individually

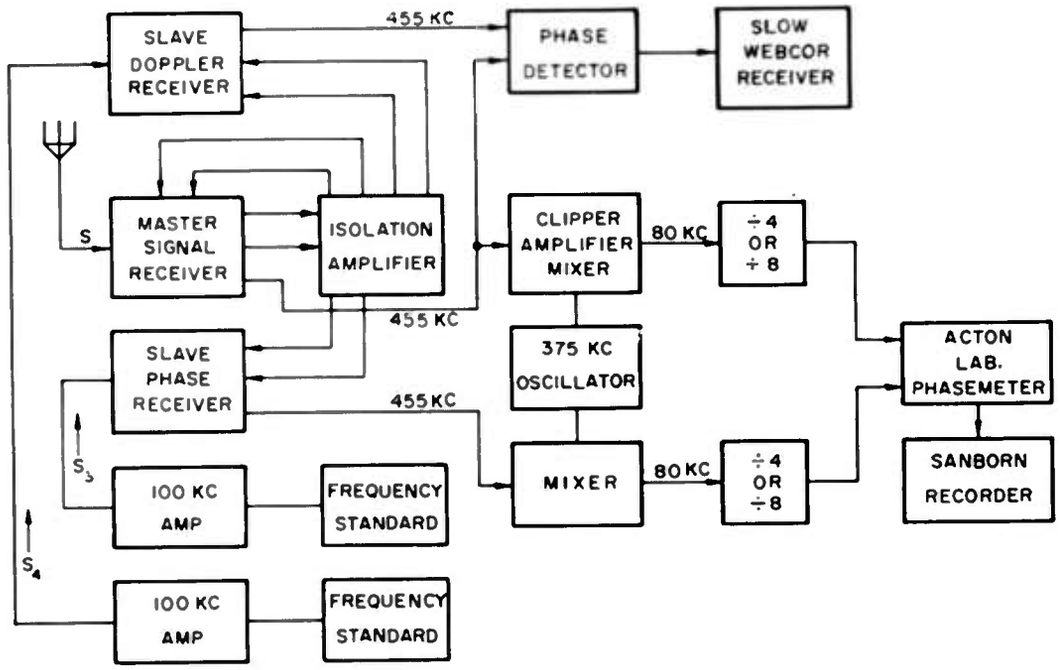

FIG. 4. TYPICAL OF TWO RECEIVING SYSTEMS

heterodyned down to a nominal 80 kc in two stages. This is accomplished with common oscillators having isolated outputs so that the 80 kc signals retain the precision phase difference $\Delta\phi = \phi_3 - \phi_1 + 2\vartheta_o H$. At this point, the signals are individually (frequency) divided by four to nominal values of 20 kc which is within the operating frequency of the Acton phasemeter. The phasemeter output is a voltage proportional to $\frac{\Delta\phi}{4} = \frac{\phi_3 - \phi_1}{4} + \frac{\vartheta_o H}{2}$. Since $\frac{\phi_3 - \phi_1}{4}$ is arbitrary and can be suppressed, we see that the time varying portion of the phasemeter is a direct analog of $H(t)$. As noted in the figure, division by eight is also available, allowing two basic levels of system sensitivity. Details of sensitivities and scale factors are considered in another section and will not be further discussed here. Note that in the presence of a strong ground wave, $S \approx S_2 = A_2 \cos(\omega t + \phi_2)$ and the phasemeter output provides a true indication of the difference in frequency between the frequency standards. The presence of a daily ground wave permitted continuous checks on stability of the standards.

An additional feature of the system was the Doppler or offset frequency comparison. The offset frequency standard was tuned to provide a reference signal (S_4) several cycles-per-second away from S_3. This signal is received and processed in a manner similar to that described above. The i-f form of S_4 can be expressed as $A_4\cos(\omega_4 t + \phi)$ while the i-f form of S_1 is of the form $A_1\cos(\omega t - 2\vartheta_o H)$. The sum of these two signals is detected and fed into a slow speed tape recorder. The recorder input has the form $A\cos[(\omega_4 - \omega)t + 2\vartheta_o H + \gamma) = A\cos(\Delta\omega t + \alpha)$. $\Delta\omega$ is the (precision) frequency difference resulting from off-setting one standard and is the frequency of a precision carrier which is phase modulated by variations in H. $\Delta\omega$ was made as small as possible, consistent with the low frequency response limitations of the recorder.

4. Phase-Height Parameters

Phase height (i.e., phase path length) was measured as a function of time. There were eight possibilities for received signals; ordinary and extraordinary waves on each of the four frequencies: 2.0, 2.2, 4.0, and 4.4 Mc. Two phase height parameters were received and recorded simultaneously in various pair combinations. The 2.0/2.2 Mc and the 4.0/4.4 Mc combinations were to provide redundancy in the event of broadcast interference. By this technique, it was intended that a "low" frequency and a "high" frequency be kept available for the experiment. The equipment did not function well at 2.0 Mc and occasional broadcast interference was experienced at 4.4 Mc, so it turned out that almost all of the records obtained were combinations of 2.2 Mc and 4.0 Mc signals. In addition, the daylight signal on 2.2 Mc contained a strong component of ground wave. Data acquisition tended to adhere to the following pattern: 1) During daylight hours and into the early evening, recorded parameters were usually 4.0 Mc ordinary and extraordinary phase height. 2) When the critical frequency of the ionosphere passed below 4.0 Mc, the equipment was switched over to 2.2 Mc ordinary and extraordinary. 3) When this signal reverted back to a ground wave sometime after sunrise, the equipment was switched back to 4.0 Mc again. 4) On some occasions, various combinations of 2.2 Mc versus 4.0 Mc signals were recorded simultaneously.

B. MAGNETIC MEASUREMENTS

The magnetic measurements were made entirely with equipment provided by Pacific Naval Laboratories at Victoria, B. C. The parameters required for the experiment were: 1) Total magnetic field, and 2) Two components of magnetic micropulsations, true north (X) and true East (Y). These will be considered in order.

1. Total Magnetic Field

Total magnetic field was measured by a rubidium vapor magnetometer. Functioning of the equipment was erratic and the output signal was very noisy to the extent that signal sensitivity was limited to about three gammas. This defect was not prohibitive since the total field was largely used as a qualitative check on the micropulsation signals. The magnetometer signal, along with the X and Y components of micropulsation signals provided sufficient information to determine amplitudes and polarizations of magnetic micropulsations.

2. Magnetic Micropulsations

The magnetic micropulsation parameters were true (geographical) North (X) and true (geographical) East (Y). The transducers employed were of the inductor type, and as such, did not have a uniform response over the frequencies of interest. The response of the equipment peaked sharply at about 0.5 cps, and fell off at about 20 db per decade at lower frequencies. The effect of this non-uniformity was that system gain had to be adjusted for the stronger signals appearing at 0.5 cps with the result that low frequency signals were extremely weak. The effect of this problem on interpretation of results is discussed more fully in the next section.

C. ATMOSPHERIC PRESSURE MEASUREMENTS

A microbarograph was set up to record atmospheric pressure waves in the region of one millibar amplitude and 2-20 minute periods. The actual range scales employed were 0.02 psi and 0.064 psi, and the low frequency limit of the equipment was estimated to be $(20 \text{ minutes})^{-1}$. Associated with the signal output of the equipment was a drift, probably thermal in nature, with a peak to peak amplitude of about 0.1 psi and a period of about 24 hours.

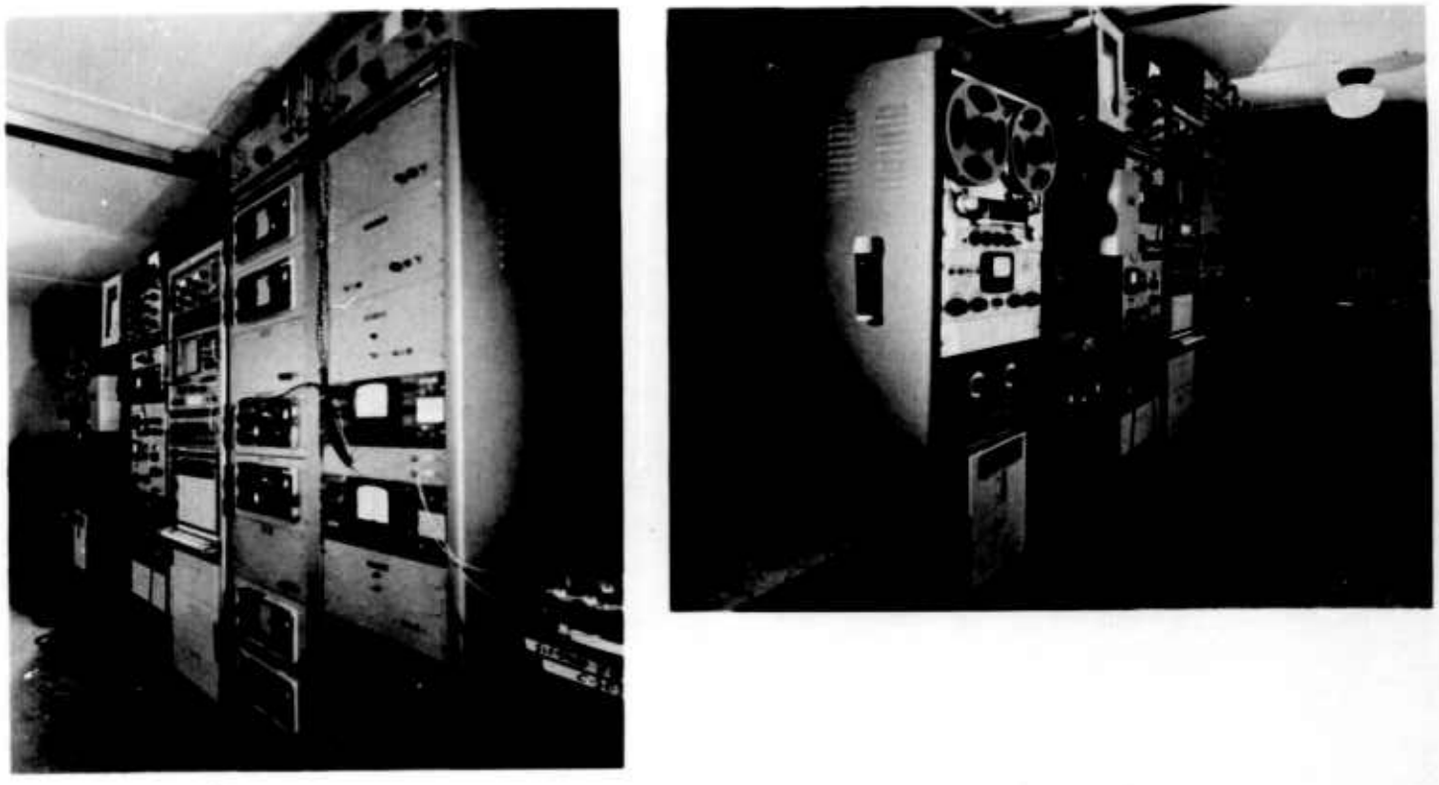

FIG. 5. INTERIOR OF RECORDING SITE

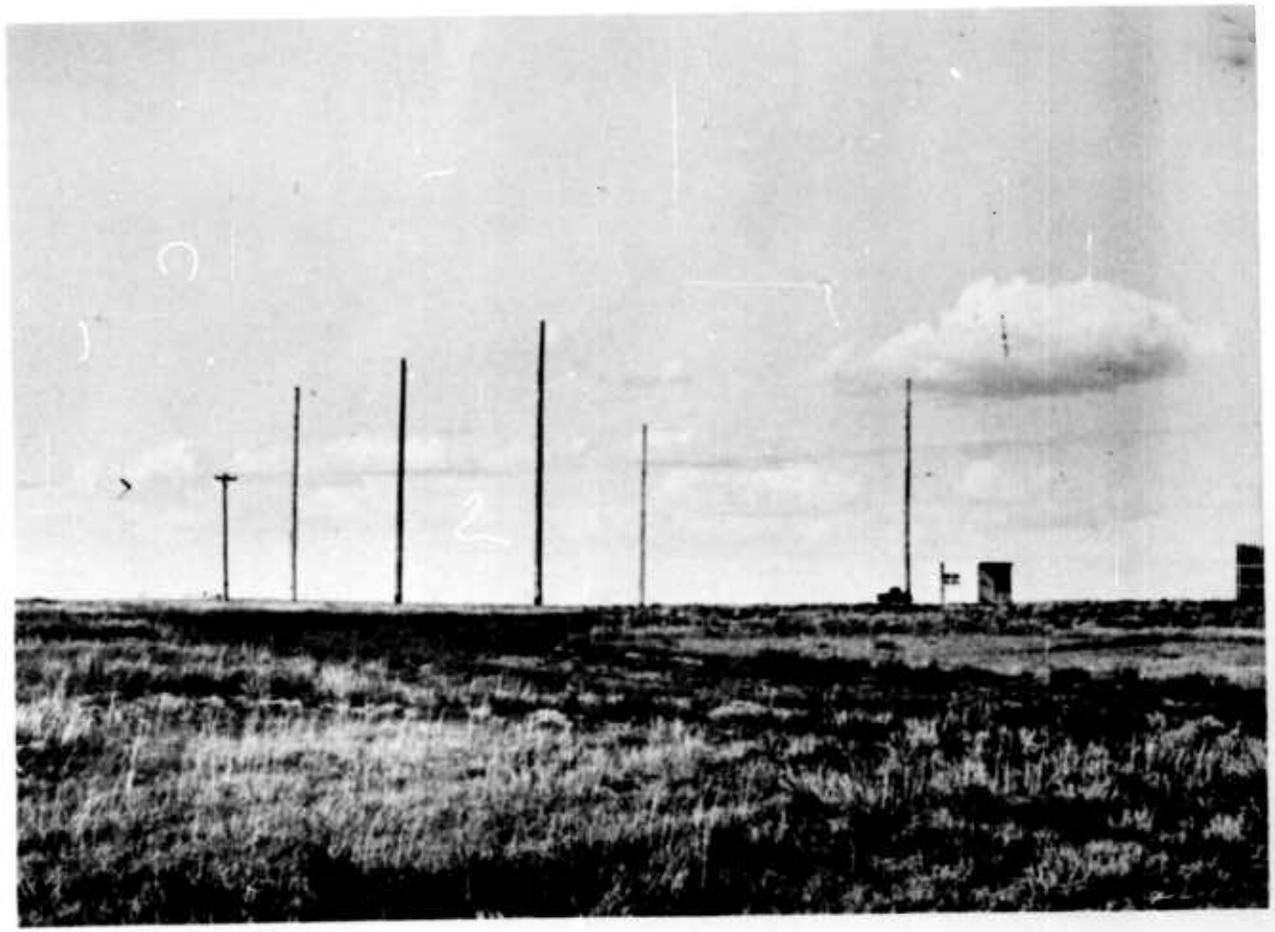

FIG. 6. TRANSMITTER SITE

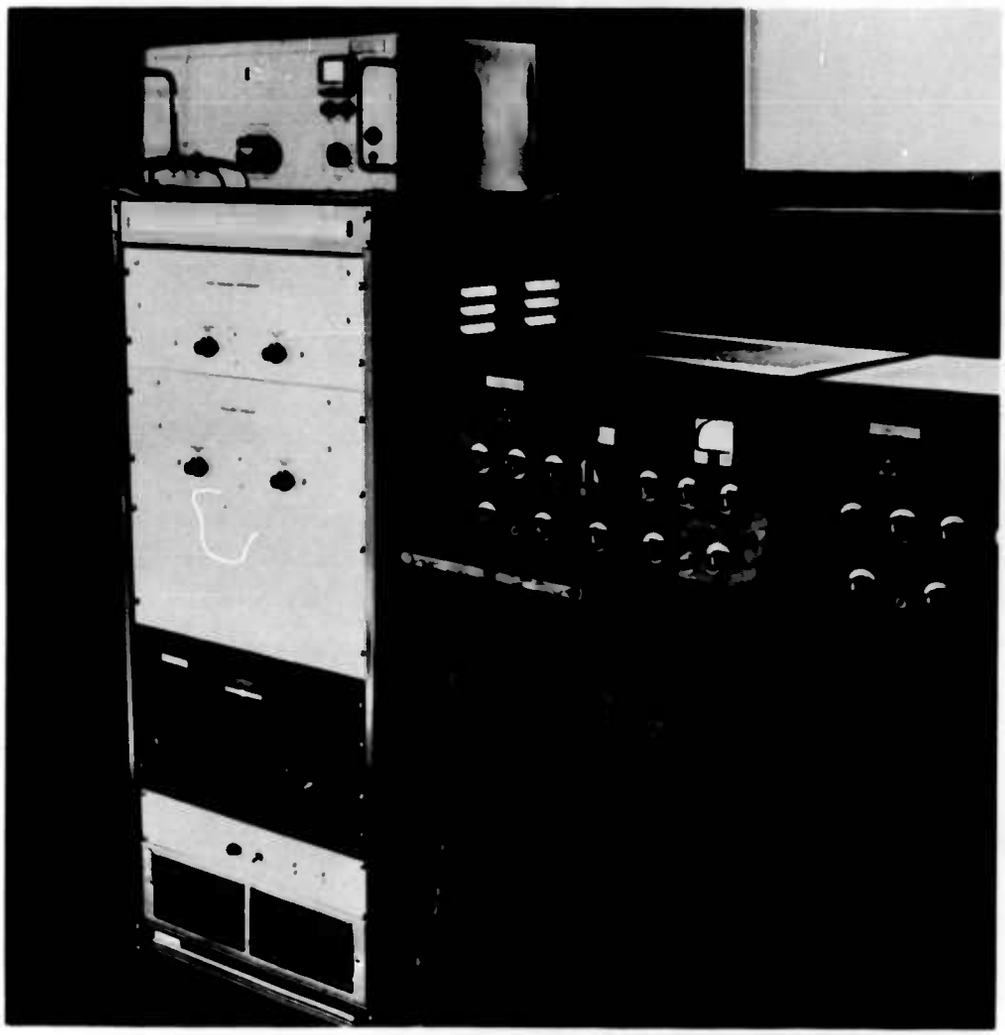

FIG. 7. INTERIOR OF TRANSMITTER BUILDING SHOWING FREQUENCY STANDARD, FREQUENCY SYNTHESIZER AND TRANSMITTER.

FIG. 8. RECEIVING SITE

III. INTERPRETATION OF RESULTS

The experiment yielded a considerable amount of data. It was necessary therefore to limit the scope of the analysis to those areas of the data most likely to yield interesting and useful results. For this reason, the interpretation of results was limited to three major areas; 1) Phase height and micropulsations, 2) Phase height and atmospheric pressure, and 3) Ordinary wave and Extraordinary wave phase height. The first of these represents the primary justification for the experiment; consequently, most of the effort has been expended in this area. The three areas are considered separately in the following sections.

A. PHASE HEIGHT AND MICROPULSATIONS

A plot of ordinary-wave and extraordinary-wave phase height and the peaks of the 'X' component (N - S) of micropulsations is shown in Figure 9 for a three-hour period on July 16, 1963. Approximately sixty percent of the micropulsation peaks appeared to correlate with phase height data. This correlation occured early in the experiment and was very encouraging. Unfortunately, this degree of correlation was not attained at any other time during the course of the experiment.

In attempting to establish correlation between phase height fluctuations and magnetic micropulsations, it is instructive to consider the relative amplitudes of signals one should expect to observe on the records. The derivation of an appropriate prediction involves essentially two steps; 1) prediction of the relative characteristics of the physical quantities themselves and 2) description of the measuring equipment and its effect on the measured quantities. These steps will now be considered in order.

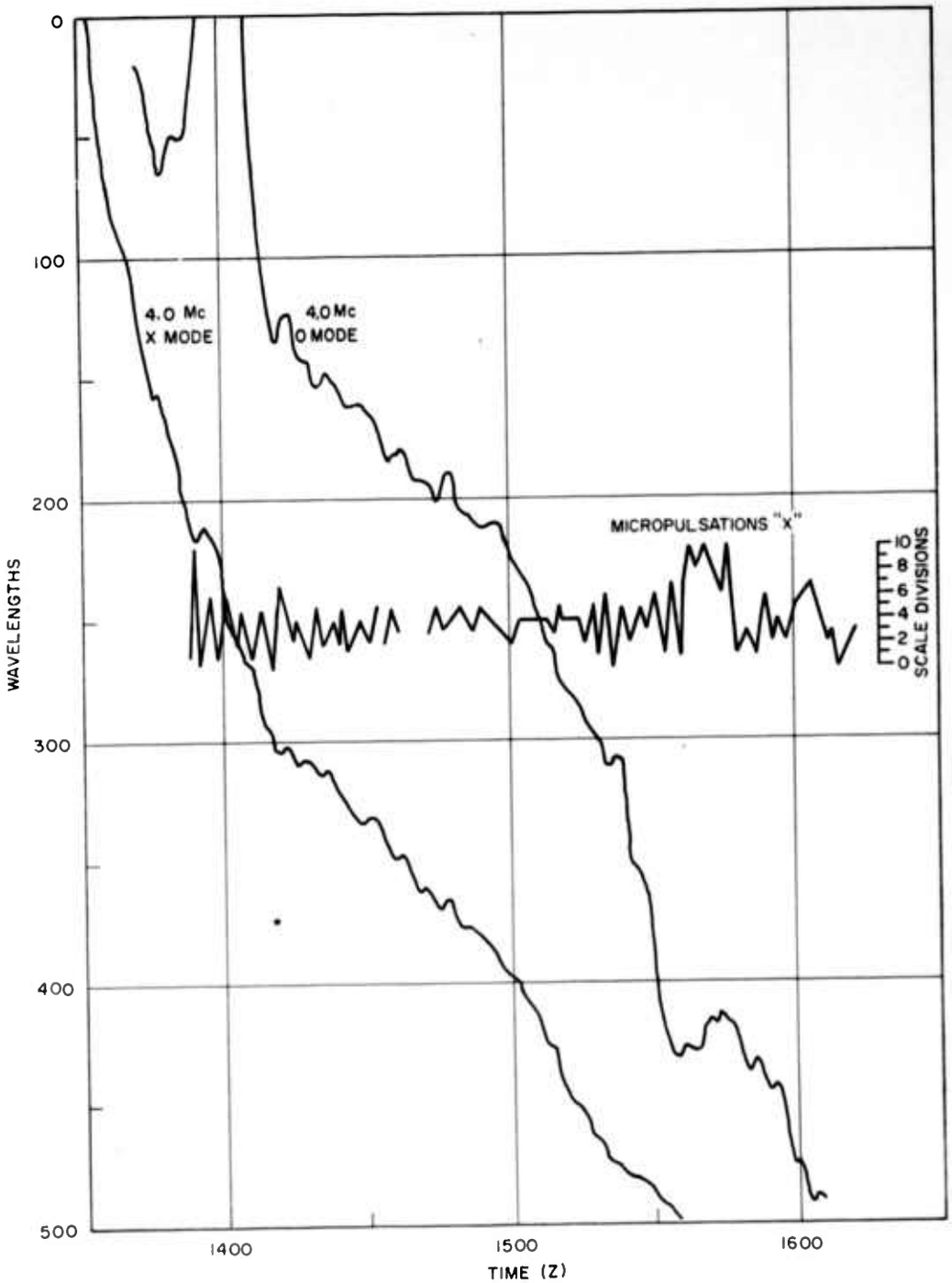

FIG. 9. PHASE HEIGHT VS MICROPULSATIONS, JULY 16, 1963

1. Physical Quantities

The most conclusive observation of these phenomena appears to be the experiment described in the report by Chan. As noted in the report, correlation was observed between magnetic micropulsations and frequency excursions about a standard frequency, which, under certain assumptions, can be interpreted in terms of vertical motion of a region of the ionosphere.

In their paper, Rishbeth and Garriott derive three independent expressions for vertical velocity. Of these, V_{ZR} is shown to follow directly from the assumptions and approximations made by Chan (i.e., mirror reflection, two-hop propagation, etc.) and is linearly related to the observed frequency excursions. Two other expressions, V_{ZM} and V_{ZH}, are developed from theory and each shows a linear relationship between vertical velocity and magnetic micropulsations. In Table 2 of their paper, these quantities are tabulated and compared with some of Chan's observations. The table is repeated here for easy reference. An additional parameter, $V_{ZR}/\Delta B$, has also been included.

Table 2

Table 1 Ref.	Approx. Local Time hr.	Period of Osc. T. min.	Freq. Devn. Δf c/s	Horiz. Mag. Devn. ΔB (Fr) γ	V_{ZR} m/s	V_{ZM}	V_{ZH}	$\frac{V_{ZR}}{\Delta B}$
E	11	.56	0.3	1.4	5	0.6	1.8	3.56
G	12	0.7	0.4	0.4	5	0.2	0.6	12.5
A	13	2.1	0.6	2	8	0.9	1.0	4.0
B	15	3.2	0.8	3.2	11	2.0	1.5	3.44
F	17	4.7	1.1	2.4	8	5	1.0	3.33
H	18	6	0.8	1.5	6	4.5	0.8	4.0
C	19	1.3	0.5	0.5	6	1.0	0.6	12.0
D	21	3.7	0.7	2	10	12	1.8	5.0
J	22	15	0.6	1.5	8	9	0.6	5.33

Examination of the values listed for $V_{ZR}/\Delta B$ (m/s per γ) reveals that seven of the nine values are reasonably self consistent with a mean of about 4 m/s per γ, more or less independent of the perturbation period. With the further assumption that Chan's micropulsation equipment had a "flat" response over the range of frequencies involved, we may conclude that the ratio of amplitudes of the physical quantities themselves does not vary with perturbation period. For the purposes of this exercise, the value 4m/s per γ will be considered representative.

Based on the foregoing, we can say

$$\Delta P_a = 2(\text{height change}) = 2\int_{\Delta t} V_{ZR}\, DT \qquad (11)$$

where Δt is the time interval of interest, and subscript "a" refers to actual values.

If we assume (for simplicity) sinusoidal variations, and let $\Delta B_a = \Delta B_a \cos \omega t$, then $V_{ZR} = 4\Delta B_a \cos(\omega t + \phi)$

$$\text{and } \Delta P_a = 2\int 4\Delta B_a \cos(\omega t + \phi)dt = \frac{8\Delta B_a}{\omega}\sin(\omega t + \phi) \qquad (12)$$

Disregarding phase, the ratio of peak values (F_a) is given by

$$F_a = \frac{\Delta P_a}{\Delta B_a} = \frac{8}{\omega} \text{ meters/gamma} \qquad (13)$$

Moreover, if we let $\omega = 2\pi/T$, then

$$F_a = \frac{\Delta P_a}{\Delta B_a} = \frac{4T}{\pi} \text{ meters/gamma} \qquad (14)$$

Subject to the various assumptions made, F_a is the actual quantity of interest.

2. Measuring Equipment

There were essentially three pieces of equipment pertinent to this portion of the experiment; the phase sounder, the micropulsation gear, and the Sanborn recorder.

a) The phase sounder output was a signal proportional in amplitude to the path length measured in units of the wavelength of the operating frequency. As part of the detailed mechanics of the system, the signal was routed through a unit which performed a "by 4" or "by 8" division at all times. The phase sounder-recorder combination was set up to have the following scale factor (S_p):

$$S_p = \frac{40}{\lambda N} \text{ divisions/meter} \tag{15}$$

where λ = wavelength of operating frequency
N = signal division factor (4 or 8)

so that

$$\Delta P_r = (S_p)(\Delta P_a) = \frac{40(\Delta P_a)}{\lambda N} \tag{16}$$

where subscript "r" refers to recorded values. For the usual conditions of 4 Mc operating frequency and $N = 4$, we have $\lambda = 75$ meters, and

$$\Delta P_r = S(\Delta P_a) = \frac{40}{4(75)} (\Delta P_a) = \frac{\Delta P_a}{7.5} \text{ Sanborn record divisions} \tag{17}$$

b) The scale factor for the Sanborn recorder-micropulsation gear combination (S_m) was determined from a frequency response calibration of the equipment. The inverse scale factor $G_m = \frac{1}{S_m}$ is plotted in Fig. 10. Then

$$\Delta H_r = (S_m)(\Delta B_a) = \frac{\Delta H_a}{G_m} \text{ Sanborn record divisions} \tag{18}$$

Although we cannot conveniently describe G_m analytically, we can express the ratio $F_r = \frac{\Delta P_r}{\Delta B_r}$.

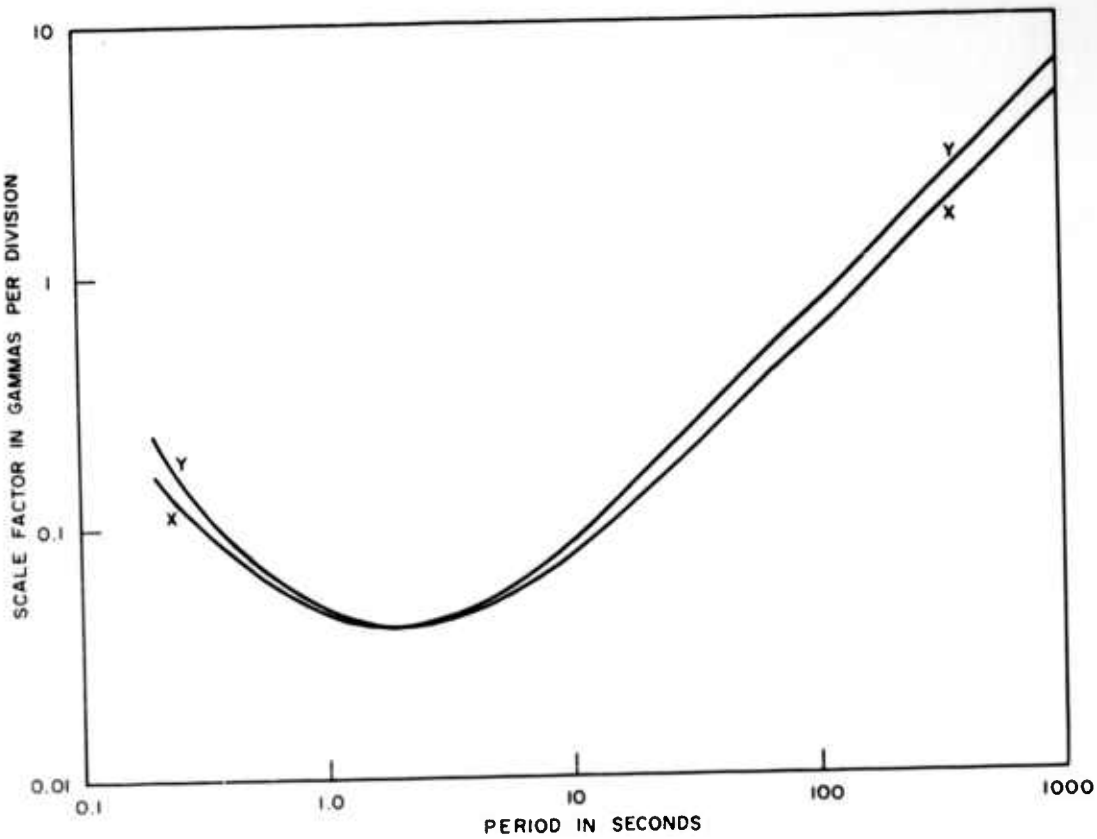

FIG. 10. MICROPULSATION SCALE FACTOR

$$F_r = \frac{\Delta P_r}{\Delta B_r} = \frac{40(\Delta P_a)}{\lambda N} \times \frac{G_m}{\Delta B_a} = \frac{40G_m}{\lambda N} \times \frac{\Delta P_a}{\Delta B_a} = \frac{40G_m F_a}{\lambda N} = \frac{160G_m T}{\pi \lambda N} \quad (19)$$

The function F_r describes the ratio of peak values of correlated signals which one might expect to observe on the records, if such correlated signals are present.

Four typical cases are plotted in Fig. 11.

(1) f = 4 Mc (λ = 75) and N = 4

(2) f = 4 Mc and N = 8

(3) f = 2 Mc (λ = 150) and N = 4

(4) f = 2 Mc and N = 8

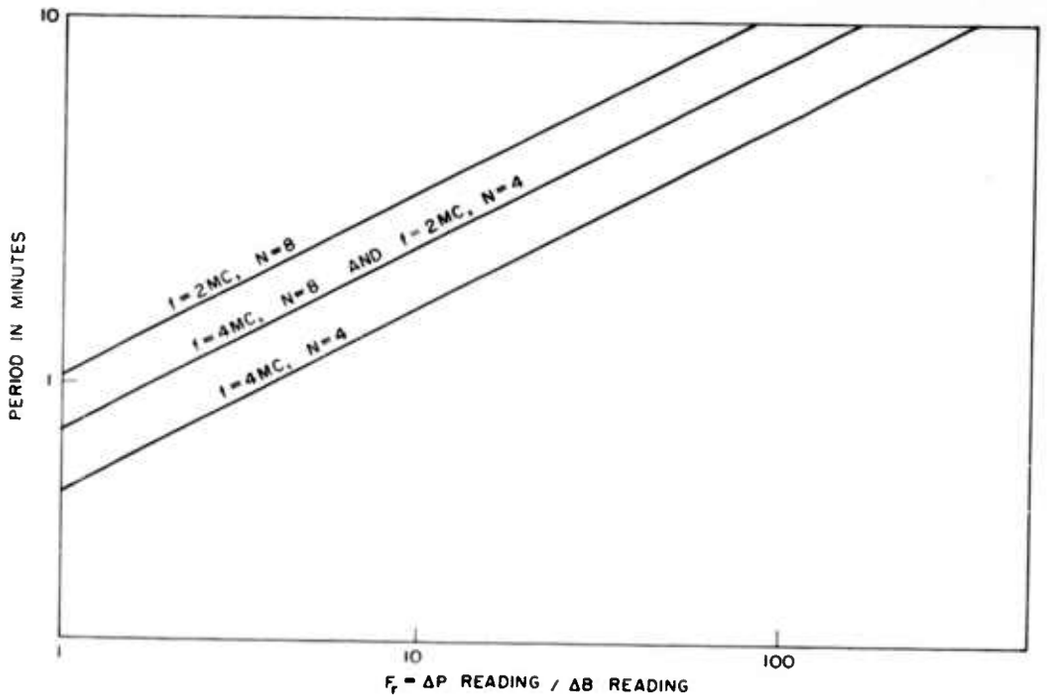

FIG. 11. CORRELATION AMPLITUDE RATIO FROM EXPERIMENTAL DATA

B. PHASE HEIGHT VERSUS ATMOSPHERIC PRESSURE

As noted earlier, theory predicts the existence of atmospheric pressure waves of extremely low frequency. As pointed out by Hines, the postulation of such waves provides an adequate interpretation of various observed phenomena such as TID's and meteor trail distortions. The gravity waves can propagate in any direction with both transverse and longitudinal components of perturbation. The vertical components of such perturbations would result in vertical oscillations of the ionospheric plasma which in principle could be detected by a vertical incidence sounder. The pressure oscillations associated with such waves could be detected through the use of a microbarograph. Unfortunately, typical vertical phase

velocities (tens of meters per second) suggest that correlation of atmospheric disturbance effects might be prevented by the great time delay involved. In addition, pressure oscillations observed at a single location provide no information with regard to phase velocity, wavelength, or direction of wave normal.

The outstanding characteristic of any wave which should be evident in any of its manifestations is that of frequency of oscillation. Correlation could exist in the following manner; a propagating gravity wave should cause plasma motion at ionospheric heights and pressure variations at ground level.

It would be extremely difficult to predict with any degree of accuracy the relative amplitudes of the two parameters one might expect to measure. It is interesting to note, in this regard, that a pressure measurement detects a wave through its compressional characteristics which are associated with longitudinal motion of the medium. Meteor trail observations, however, indicate that gravity waves at ionospheric heights are characterized primarily by transverse motions of the medium.

An additional factor to be considered is that the origin of gravity waves is not well understood. Without knowing where a wave originated, the time delay between two spatially separate measurements cannot be predicted.

In Fig. 12 is shown a typical plot of atmospheric pressure variations and 4.0 Mc Ordinary wave phase height variations, both as functions of time. No correlation was detected from this plot, nor was any correlation detected from any of the data.

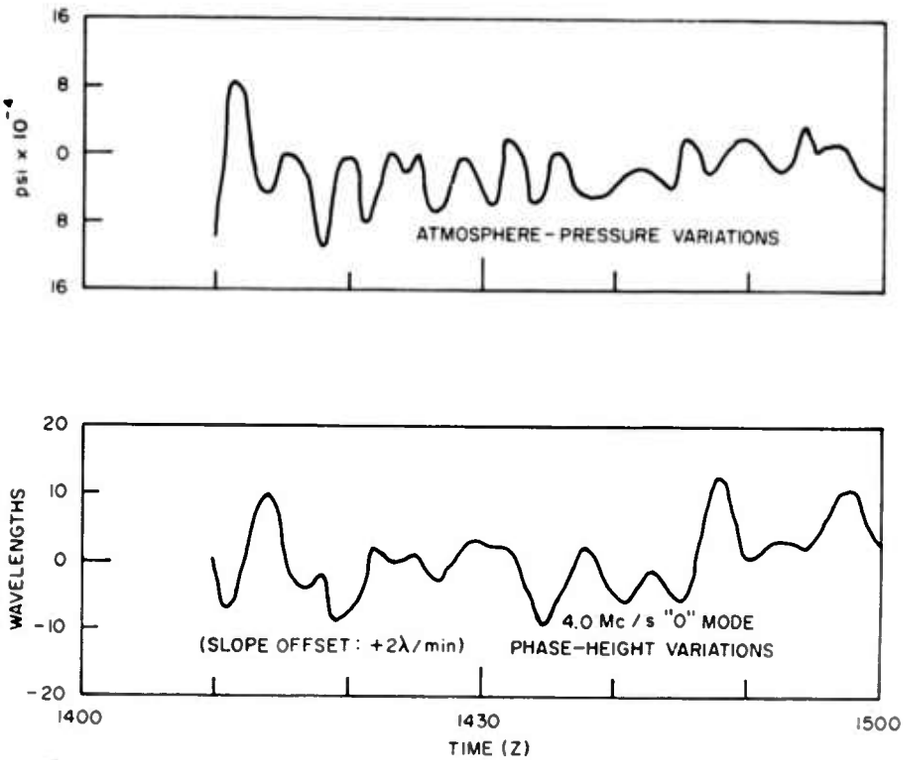

FIG. 12. TYPICAL COMPARISON OF PHASE HEIGHT AND ATMOSPHERIC PRESSURE VARIATIONS

C. ORDINARY WAVE VS EXTRAORDINARY WAVE PHASE HEIGHT

Through the use of crossed dipole antennas and hybrid transformer units, the phase sounder receiver was able to receive separately and simultaneously both the Ordinary (O) and Extraordinary (X) components of the reflected wave. According to the magnetoionic theory, the ray paths of O and X waves diverge upon entering the ionosphere so that the reflected components of these separate waves represent reflection from different regions of the ionosphere. It has been

shown by Budden[4] (1961) and elsewhere that the ray path of a vertically incident wave lies in a plane defined by the magnetic meridian. In the case of vertical incidence which is appropriate to this experiment, the ray paths are approximately as shown in Fig. 13 in which the reasonable assumption is made that collision frequencies are much smaller than the wave frequency. As seen in the sketch, the points of reflection of the two waves differ both in latitude and elevation.

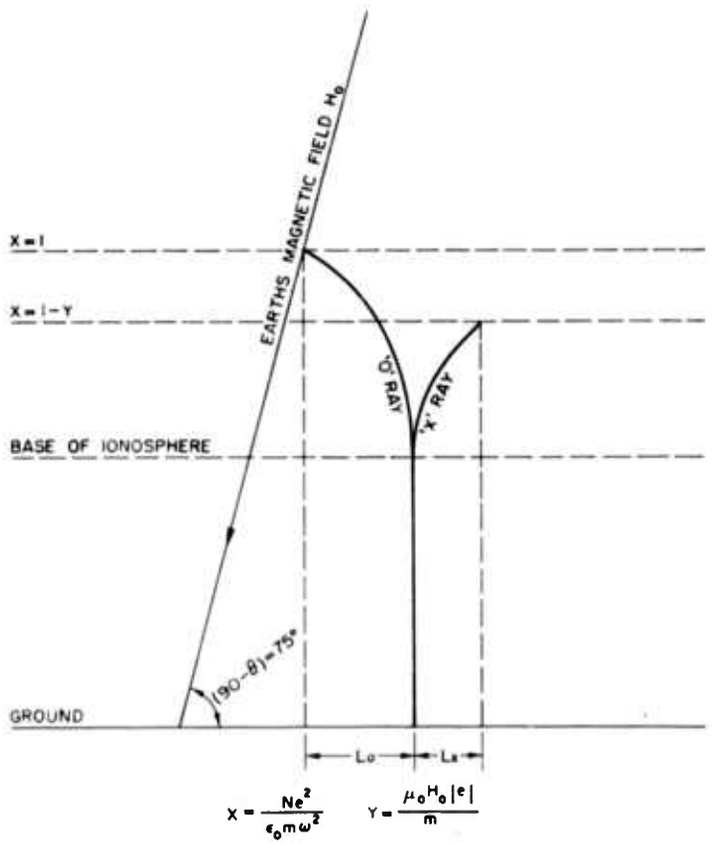

FIG. 13. ORDINARY AND EXTRAORDINARY RAY PATHS

It is instructive to consider the latitudinal separation between the reflection heights of the Ordinary and the Extraordinary wave. If we assume vertical incidence and no collisions, we can make use of equation 13.44 in Budden as follows:

$$\frac{\partial l}{\partial z} = \phi = \frac{\sin\theta \cos\theta\, Y^2(1 - \mu^2)}{\left\{4Y_L{}^2(1 - X)^2 + Y_T{}^4\right\}^{\frac{1}{2}}} \qquad (20)$$

in which ϕ is the angle between the ray path and the vertical, l is a horizontal coordinate in the magnetic meridian, and z is a vertical coordinate.

If we let dl equal the incremental lateral deviation of a ray, then we can say $dl = (\frac{\partial l}{\partial z})dz$ and

$$L_o = \int_o^{L_o} dl_o = \int_o^{Z_o} (\frac{\partial l_o}{\partial z})dz \quad \text{for the ordinary wave} \qquad (21)$$

$$L_x = \int_o^{L_x} dl_x = \int_o^{Z_x} (\frac{\partial l_x}{\partial z})dz \quad \text{for the extraordinary wave} \qquad (22)$$

where Z_o and Z_x are the heights of reflection for the respective waves.

Substituting (20) into (21) and (22), we obtain

$$L_o = \int_o^{Z_o} \frac{\sin\theta \cos\theta\, Y^2(1 - n_o{}^2)}{\left\{4\, Y_L{}^2(1 - X)^2 + Y_T{}^4\right\}^{\frac{1}{2}}}\, dz \qquad (23)$$

$$L_x = \int_o^{Z_x} \frac{\sin\theta \cos\theta\, Y^2(1 - n_x{}^2)}{\left\{4\, Y_L{}^2(1 - X)^2 + Y_T{}^4\right\}^{\frac{1}{2}}}\, dz \qquad (24)$$

We will use a Chapman model ionosphere, so for convenience, we make a vertical translation of our coordinate system so that vertical distance is measured with the peak of the layer considered as the origin. Because in the Chapman model the electron concentration is negligible at distances greater than three scale heights below the peak, the integration lower limit is set at minus three scale heights. A reasonable value for daytime scale height is 80 km, so our lower limit becomes 240 km. We then have

$$L_o = \int_{-240}^{Z_o} \frac{\sin \theta \cos \theta \, Y^2(1 - n_o^2)}{\left\{4 Y_L^2(1 - X)^2 + Y_T^4\right\}^{\frac{1}{2}}} \, dz \qquad (25)$$

$$L_x = \int_{-240}^{Z_x} \frac{\sin \theta \cos \theta \, Y^2(1 - n_x^2)}{\left\{4 Y_L^2(1 - X)^2 + Y_T^4\right\}^{\frac{1}{2}}} \, dz \qquad (26)$$

where z is a coordinate directed upward from the peak of the Chapman layer. The various functions appearing in the integrals are standard magnetoionic parameters and are defined below as by Ratcliffe[5] (1959):

$$Y = \frac{\mu_o H_o |e|}{\omega m} \qquad (27)$$

$$Y_L = Y \cos \theta \qquad (28)$$

$$Y_T = Y \sin \theta \qquad (29)$$

$$X = \frac{Ne^2}{E_o m \omega^2} \qquad (30)$$

From the Appleton-Hartree equations, we have

$$n_o^2 = 1 - \frac{X}{1 - \frac{1}{2}\left(\frac{Y_T^2}{1 - X}\right) + \left[\frac{1}{4}\,\frac{Y_T^4}{(1 - X)^2} + Y_L^2\right]^{\frac{1}{2}}} \qquad (31)$$

$$n_x^2 = 1 - \frac{X}{1 - \frac{1}{2}\left(\frac{Y_T^2}{1 - X}\right) - \left[\frac{1}{4}\,\frac{Y_T^4}{(1 - X)^2} + Y_L^2\right]^{\frac{1}{2}}} \qquad (32)$$

The Chapman layer is defined by

$$N = N_{max} \exp\left[\frac{1}{2}\left\{1 - Z/H - \exp(-Z/H)\right\}\right] \qquad (33)$$

The value of N_{max} is determined from the following considerations: (1) Reflection of the ordinary wave occurs where $X = 1$, that is where the plasma frequency of the medium becomes equal to the wave frequency. (2) Associated with the layer is some maximum frequency at which the ordinary wave can be reflected at vertical incidence. If we designate this frequency as f_{max} and define $\omega_{max} = 2\pi(f_{max})$, then N_{max} is determined directly from equation (30) as:

$$X = 1 = \frac{N_{max}\, e^2}{\epsilon_o\, m(\omega_{max})^2}\,, \qquad (34)$$

hence

$$N_{max} = \frac{\epsilon_o\, m(\omega_{max})^2}{e^2} \qquad (35)$$

From the condition that the Ordinary wave reflects at $X = 1$ and the Extraordinary wave reflects at $X = 1 - Y$ (see Ratcliffe) we can determine Z_o and Z_x, the upper limits of our two integrals. To determine Z_o, we set $X = 1$ and $z = Z_o$ and combine equations (30), (33) and (35), whence;

$$X = 1 = \frac{Ne^2}{\epsilon_o m\omega^2}\left[\frac{\epsilon_o m(\omega_{max})^2}{e^2}\right] \exp\left[\tfrac{1}{2}\left\{1 - Z_o/H - \exp(-\frac{Z_o}{H})\right\}\right]$$

from which is obtained

$$\frac{Z_o}{H} + \exp(-\frac{Z_o}{H}) = 1 - 2\log\frac{\omega^2}{(\omega_{max})^2} \qquad (36)$$

Similarly, for Z_x we have $X = 1 - Y$, $z = Z_x$, and

$$1 - Y = \frac{e^2}{\epsilon_o m\omega^2}\left[\frac{\epsilon_o m(\omega_{max})^2}{e^2}\right] \exp\left[\tfrac{1}{2}\left\{1 - \frac{Z_x}{H} - \exp(-\frac{Z_x}{H})\right\}\right]$$

which leads to

$$\frac{Z_x}{H} + \exp(-\frac{Z_x}{H}) = 1 - 2\log\left[\frac{(1 - Y)\,\omega^2}{(\omega_{max})^2}\right] \qquad (37)$$

Equations (36) and (37) each have two solutions; that is, for any $\frac{\omega}{\omega_{max}} < 1$, each equation has one positive and one negative solution for $\frac{Z_{o,x}}{H}$. The physical reason for this is that for any value of N $(N < N_{max})$ in the layer, there is one point above the peak and one point below the peak where such a value of N can be found. Since we are concerned only

with the region below the peak, only negative values of $\frac{Z_{o,x}}{H}$ are considered.

The geography of the experiment determined the values $\theta = 15^{o}$ and $\mu_o H_o = 0.601 \times 10^{-4}$ webers/m^2. Using a radio frequency of 4.0 Mc and a variety of representative values for f_{max}, solutions to equations (25), (26), (36) and (37) have been obtained through the use of a high speed digital computer. Integrals (25) and (26) have been solved in iterative form, yielding a complete ray path profile for each combination of parameters, although only the values for Z_o, Z_x, L_o, and L_x are of immediate interest.

These results have been tabulated in Table 2 where values of the quantities have been found for various values of f_{max} and a fixed wave frequency $f = 4.0$ Mc.

Table 2

f_{max}(Mc)	Z_o(km)	Z_x(km)	L_o(km)	L_x(km)	L_o+L_x(km)
4.05	- 24	- 97	47.58	3.50	51.08
4.5	- 67	-110	20.53	2.99	23.52
5.0	- 88	-120	13.71	2.58	16.29
5.5	-101	-128	9.49	2.36	11.85
6.0	-111	-135	8.14	2.27	10.41

The situation is a realistic one; variations in N_{max} give rise to a proportionate variation of f_{max}, according to equation (35). It can be seen that for transmitting frequencies very close to the critical frequency, the quantity $(L_o + L_x)$ is quite sensitive to changes in the critical frequency. An accurate determination of the parameter $(L_o + L_x)$ would require the use of an ionosound or other means to provide a continuous measurement of f_{max}.

A close inspection of Fig. 14 reveals that the two phase height curves are generally similar but that much of the fine structure is not coincident in time. This suggests traveling waves and leads to the conclusion that this technique can be used as a means of studying traveling disturbances in the ionosphere. Davies[6] (1962) has commented on this technique and noted the precautions which should be observed in the interpretation of results.

IV. CONCLUSIONS

As noted earlier, the experiment had three aspects, which were essentially independent. The comparison of phase height with micropulsations was the primary justification for the experiment. The other two aspects, comparison of phase height with atmospheric pressure and comparison of Ordinary wave and Extraordinary wave phase height, were pursued insofar as they did not interfere with the primary consideration. Nevertheless, conclusions can be drawn for each part of the experiment, and these will now be considered in order.

A. COMPARISON OF PHASE HEIGHT AND MICROPULSATIONS

The purpose of this portion of the experiment was to look for correlation between ionospheric phase height fluctuations and long period magnetic micropulsations. Such correlation was observed in an experiment by Chan, and an interpretation of the correlation has been suggested by Rishbeth and Garriott as noted earlier. Inasmuch as observed correlation has been rare, the experiment herein described was intended to provide experimental evidence of this interesting phenomena.

The observations were inconclusive. Positive correlation was not observed, yet it is impossible to conclude that such

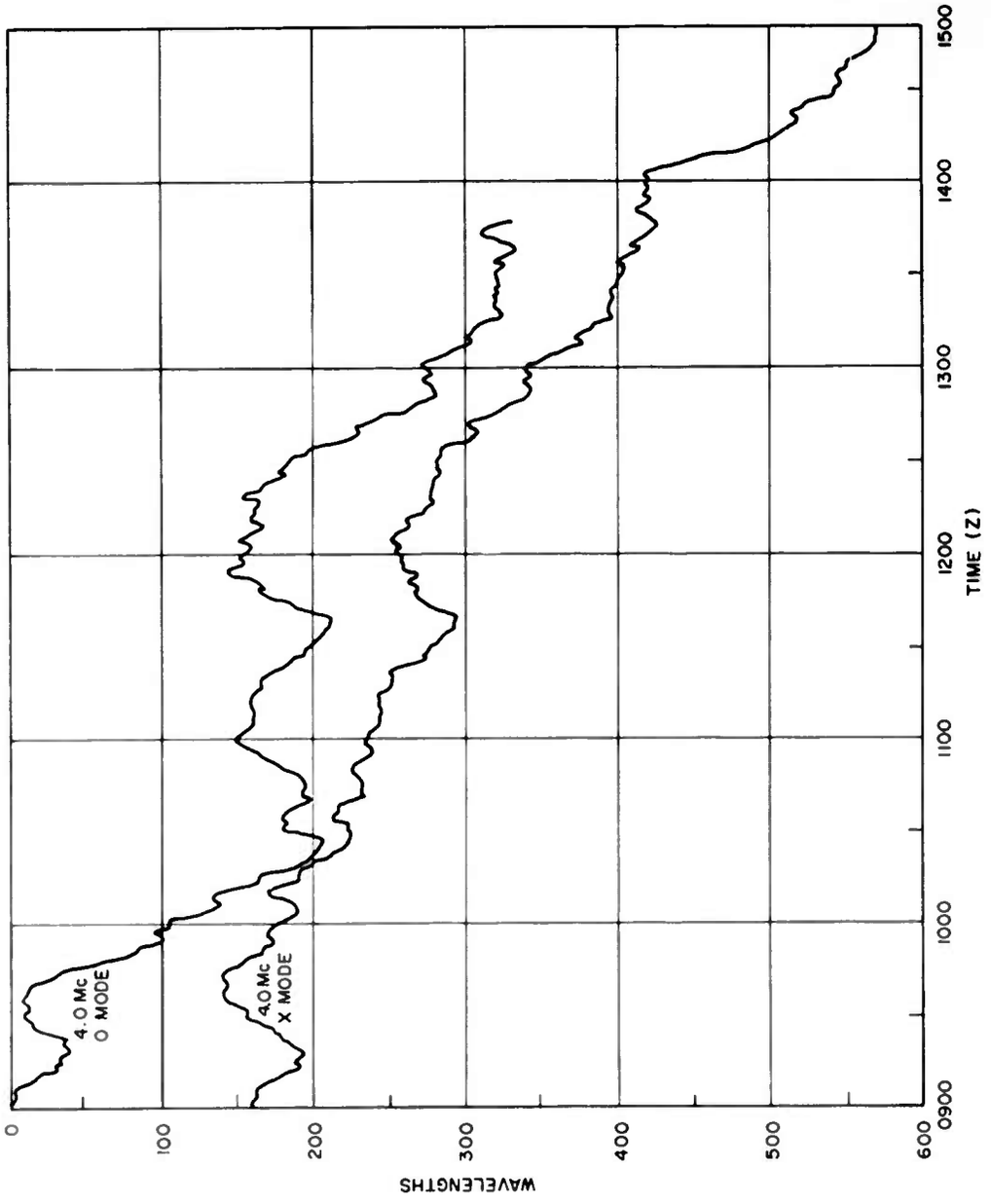

FIG. 14. ORDINARY AND EXTRAORDINARY PHASE HEIGHT, JULY 14, 1963

correlated physical phenomena were necessarily absent. In examining the various factors which influenced the experimental results, two of these factors have emerged as having a predominantly deteriorating effect on the experiment. These factors are as follows: 1) The response of the magnetic micropulsation equipment was not matched to the requirements of the equipment. The effect of this mismatch is explained in Section III-C, so it will not be repeated here. It might be said that the narrow bandwidth associated with the equipment used in this experiment appears to be characteristic of the coil or inductance type of instrument. In contrast, the micropulsation gear used in the Chan experiment had a uniform response to all frequencies of interest. 2) The radio equipment did not function properly at 2.0 or 2.2 Mc. The transmitter antennas were forty feet from the ground, and the results of this low height were excessive loading of the transmitter and excessive ground wave emissions. The ground wave interfered with the night-time sky wave with the result that very little useful data could be obtained on either 2.0 or 2.2 Mc.

B. COMPARISON OF PHASE HEIGHT AND ATMOSPHERIC PRESSURE

Of the three aspects of the experiment, this appears to be least promising. The biggest drawback appears to be that a given pressure fluctuation at ground level which is thought to be associated with a gravity wave provides no information with regard to direction or velocity of the gravity wave. Since the phase sounder is exploring only a small region of the ionosphere, the chance of finding correlation appears remote. This portion of the experiment was performed only because it was so easily accomplished; it involved only setting up and recording the output of a microbarograph.

C. COMPARISON OF ORDINARY-WAVE AND EXTRAORDINARY-WAVE PHASE HEIGHT

Although this aspect of the experiment has not been developed very far, the possibilities for further development and experimentation appear very good, indeed. Under the present circumstances, there are several drawbacks which should be corrected if this area of investigation were to be pursued. 1) The ionospheric model used here is a Chapman layer which is reasonably valid only under conditions of equal production and loss. 2) The parameter $(L_o + L_x)$ is of great importance and should be determined as accurately as possible. Inspection of Table A reveals the dependence of this parameter on f_{max}. For this reason, f_{max} should be determined at all times when measurements are being made. 3) A knowledge of $(L_o + L_x)$ and a measurement of the time between similar occurrences on the O and X records will provide information about one velocity component of a traveling disturbance, this component being along a line connecting the points of reflection, that is (Z_o, L_o) and (Z_x, L_x). If two receiving stations were set up on a line normal to the magnetic meridian, such an arrangement would provide monitoring of four points in the ionosphere instead of only two. These four points would very closely define a plane with the result that the velocity of any traveling disturbance could then be described in two dimensions instead of one.

BIBLIOGRAPHY

1. Hines, C. O., "Internal Atmospheric Gravity Waves at Ionospheric Heights," Canadian Journal of Physics 38, 1441 (1960).

2. Chan, K. L., "Study of Short-Period Variations in the Ionosphere by Means of Instantaneous Frequency Measurements," TR No. 66, Nonr-225(33), Stanford Electronics Laboratories, Stanford, California, October 1962.

3. Rishbeth, H., and Garriott, O. K., "Relationship Between Simultaneous Geomagnetic and Ionospheric Oscillations," Radio Science Journal of Research NBS/USNC-URSI, Volume 68D, No. 3, 339-343, March 1964.

4. Budden, K. G., "Radio Waves in the Ionosphere," Cambridge, 1961.

5. Ratcliffe, J. A., "The Magnetoionic Theory and Its Applications to the Ionosphere," Cambridge, 1959.

6. Davies, K., "The Measurement of Ionospheric Drifts by Means of a Doppler Shift Technique," Journal of Geophysical Research 67, 4909 (1962).

7. Baker, W. G., and Martyn, D. F., "Electric Currents in the Ionosphere," Phil. Roy. Soc. A246, 281 (1953).

ONR-ARPA DISTRIBUTION LIST

(Revised by ONR July 1964)

No. of Copies

NAVY

Chief of Naval Research
Department of the Navy
Washington, D. C. 20360
1 Attn: Code 402C
2 Attn: Code 418

Director
Naval Research Laboratory
Washington 25, D.C.
1 Attn: Code 5320 (Mr. J. M. Headrick)
1 Attn: Code 2027

Chief of Naval Operations
Department of the Navy
Washington 25, D.C.
1 Attn: OP-723E
1 Attn: OP-07TE

Director, Special Projects Office
Department of the Navy
Washington 25, D.C.
1 Attn: Code SP-204

Commander
Pacific Missile Range
Point Mugu, California
1 Attn: Code 3215

Commander
Naval Missile Center
Point Mugu, California
1 Attn: Code N03022

Commanding Officer and Director
U. S. Navy Electronics Laboratory
San Diego, California 92152
1 Attn: Mr. H. J. Wirth
1 Attn: Library

Commanding Officer
U. S. Naval Ordnance Laboratory
Corona, California 91720
1 Attn: Mr. V. E. Hildebrand (Code 453)

No. of Copies

AIR FORCE

Headquarters
Air Force Systems Command
Foreign Technology Division
Wright-Patterson AFB, Ohio
1 Attn: TDC (Mr. Zabatakas)
1 Attn: TDEED (Mr. W. L. Picklesimer)
1 Attn: TDATA (Mr. G. A. Long, Jr.)
1 Attn: TDCE (Mr. M. S. J. Graebner)

Headquarters, RTD
Bolling AFB
Washington, D.C. 20332
1 Attn: RTHC (Col. Richard Cosel)

Rome Air Development Center
Research and Technology Division
Griffiss Air Force Base, New York
1 Attn: EMASR (Mr. Vicent J. Coyne)
1 Attn: RAVEL-3 (Mr. G. R. Weatherup)
1 Attn: RALCS (Mr. Salvador DiGennaro)

Commander
USAF Security Systems
San Antonio, Texas
1 Attn: ODCR (Mr. Walter L. Anderson)

Headquarters, USAF
Office of Assistant Chief of Staff, Intelligence
Washington, D.C. 20330
1 Attn: AFNICAA (Lt. Col. Brubaker)

ONR-ARPA DISTRIBUTION LIST

No. of Copies

AIR FORCE

Headquarters
North American Air Defense Command
Ent AFB
Colorado Springs 12, Colorado
1 Attn: NPSD-A (Col. M. R. Cripe)
1 Attn: NELC-AP

Headquarters, AFCRL
L. G. Hanscom Field
Bedford, Massachusetts
1 Attn: CRUP (Dr. G. J. Gassman)
1 Attn: CRUI (Mr. W. F. Ring)

Headquarters, USAF
Office of Assistant Chief of Staff
for Intelligence
Policy and Programs Group, AFNINC
Washington 25, D.C.

Headquarters, SAC
Offutt AFB
Omaha, Nebraska
1 Attn: Mr. Eugene Jackson

ARMY

Chief, Army Security Agency
Arlington Hall Station
Arlington, Virginia
1 Attn: Col. James E. Helgestad

Commanding Officer
U. S. Army Material Command
Washington 25, D. C.
1 Attn: AMCRD-D

Commanding Officer
U. S. Army Munitions Command
Picatinny Arsenal
Dover, New Jersey
1 Attn: SMUPA-VA6

Commanding Officer
U. S. Army Electronics Research Unit
P. O. Box 205
Mountain View, California
1 Attn: Mr. Joseph Bert

No. of Copies

U. S. Army, SLAG
P. O. Box 7157
Apex Station
Washington, D.C. 20004
1 Attn: Mr. N. R. Garofalo

DOD

Director
Advanced Research Projects
Agency
Washington 25, D. C.
1 Attn: Mr. Alvin Van Every

Director
Weapons Systems Evaluation
Group
Office of the Director of
Defense Research and
Engineering
Washington 25, D.C.

Office of Assistant Chief of
Staff for Intelligence
Department of the Army
Room 2B457, The Pentagon
Washington 25, D.C.
1 Attn: Mr. Joseph Grady

Office of the Assistant
Director
Intelligence and Reconnaissance
Office of the Director of
Defense Research and
Engineering
Room 3E119, The Pentagon
Washington 25, D. C.
1 Attn: Mr. Howard A. Staderman

Defense Intelligence Agency
Pentagon Annex #3, Room 303
Washington 25, D. C.
1 Attn: AQ-2A (Captain James
Stewart)

ONR-ARPA DISTRIBUTION LIST

No. of Copies

DOD

Deputy Director
Research and Technology
Office of the Director of Defense
Research and Engineering
Room 3E1030, The Pentagon
Washington 25, D.C.
1 Attn: Dr. Chalmers W. Sherwin

Office of the Assistant Director
(Defense Systems)
Defense Research and Engineering
Room 3D138, The Pentagon
Washington 25, D.C.
1 Attn: Mr. Daniel Fink

Director
National Security Agency
Fort George G. Meade, Maryland
1 Attn: K-344 (Mr. Charles Gandy)
1 Attn: C3/TDL

Director
Defense Intelligence Agency
Room 1C917, The Pentagon
Washington 25, D.C.
1 Attn: DIAST-B (Mr. Thomas Brooke)

Director
Defense Intelligence Agency
Room 3B259, The Pentagon
Washington 25, D.C.
1 Attn: DIAIS-I (Col. John G. Johnson)

Defense Documentation Center
Cameron Station
Alexandria, Virginia 22314
20 Copies

OTHER

ACF-E Industries
3355-52nd Avenue
Hyattsville, Maryland
1 Attn: Mr. William T. Whelan

No. of Copies

Aero Geo Astro Corporation
13624 Magnolia Avenue
Corona, California
1 Attn: Mr. A. W. Walters

Astrophysics Research
Corporation
2444 Wilshire Blvd., Room 512
Santa Monica, California
1 Attn: Dr. Alfred Reifman

HRB Singer, Inc.
Science Park
State College, Pennsylvania
1 Attn: Library

Institute for Defense Analyses
1666 Connecticut Avenue
Washington 9, D.C.
1 Attn: Dr. Paul von Handel

Institute of Science and
Technology
The University of Michigan
P.O. Box 618
Ann Arbor, Michigan
1 Attn: BAMIRAC Library

Massachusetts Institute of
Technology
Center for Space Research
Building 33-109
Cambridge, Massachusetts
1 Attn: Dr. J. V. Harrington

Massachusetts Institute of
Technology
Lincoln Laboratory
Lexington 73, Massachusetts
1 Attn: Dr. J. H. Chisholm

MITRE Corporation-E Bldg.
Room 353
Bedford, Massachusetts
1 Attn: Mr. William A.
Whitcraft, Jr.

ONR-ARPA DISTRIBUTION LIST

No. of Copies		No. of Copies	
	OTHER		
	National Bureau of Standards Boulder Laboratories Boulder, Colorado		University of California Mathematics Department Berkeley 4, California
1	Attn: 85.20 (Mr. L. H. Tveten)	1	Attn: Dr. Edmond J. Pinney
	Pickard and Burns, Inc. Research Department 103 Fourth Avenue Waltham 54, Massachusetts		
1	Attn: Dr. John C. Williams		
	Princeton University James Forrestal Research Center Sayre Hall Princeton, New Jersey		
1	Attn: Dr. Edward Frieman		
	RAND CORPORATION 1700 Main Street Santa Monica, California		
1	Attn: Dr. Ivan Selin		
1	Attn: Dr. Cullen Crain		
1	Attn: Library		
	Raytheon Company Communication and Data Processing Operations 1415 Boston-Providence Turnpike Norwood, Massachusetts		
1	Attn: Mr. L. C. Edwards		
	Stanford Research Institute Menlo Park, California		
1	Attn: Dr. David Johnson		
	Mr. Thurston B. Soisson Box 3164 SW Station Washington, D. C.		
	Sylvania Electronics Systems Electronic Defense Laboratories P. O. Box 205 Mountain View, California		
1	Attn: Mr. John Don Carlos		

UNCLASSIFIED